

Metalloporphyrins as chemical shift reagents: the unambiguous NMR characterization of the *cis*- and *trans*-isomers of *meso*-(bis)-4'-pyridyl-(bis)-4'-carboxymethylphenylporphyrins

Teresa Gianferrara,^{a,*} Davide Giust,^a Ioannis Bratsos^b and Enzo Alessio^b

^aDipartimento di Scienze Farmaceutiche, Università di Trieste, Piazzale Europa 1, 34127 Trieste, Italy

^bDipartimento di Scienze Chimiche, Università di Trieste, Via L. Giorgieri 1, 34127 Trieste, Italy

Received 28 September 2006; revised 2 March 2007; accepted 22 March 2007

Available online 27 March 2007

Abstract—The condensation of pyrrole with 4-pyridylcarboxyaldehyde and methyl 4-formyl benzoate under Adler–Longo conditions yielded the series of *meso*-(4'-pyridyl)/(4'-carboxymethylphenyl)porphyrins as a mixture. Careful column chromatography afforded each isomer in pure form. In this paper we focus on the two bis-substituted isomeric *meso*-porphyrins, 5,10-bis(4'-pyridyl)-15,20-bis(4'-carboxymethylphenyl)porphyrin and 5,15-bis(4'-pyridyl)-10,20-bis(4'-carboxymethylphenyl)porphyrin, respectively, 4'-*cis* and 4'-*trans*DPyDMeP. The assignment of the geometry of the two isomers was performed by ¹H NMR spectroscopy on the trinuclear adducts [(4'-*cis*DPyDMeP){Ru(TPP)(CO)}₂] and [(4'-*trans*DPyDMeP){Ru(TPP)(CO)}₂], obtained by selective coordination of [Ru(TPP)(CO)(EtOH)] (TPP=tetra-phenylporphyrin) to the peripheral nitrogen atoms. The axially bound ruthenium porphyrins act as chemical shift reagents on the central porphyrin, allowing a clear distinction of the pyrrole proton resonances and consequent unambiguous assignment of the geometry of each isomer based upon symmetry considerations.

© 2007 Elsevier Ltd. All rights reserved.

1. Introduction

Porphyrins bearing electron-donor moieties in peripheral positions, such as *meso*-pyridyl/phenyl porphyrins (PyPs), are capable of exocyclic coordination to metal centres and for this reason are widely exploited in the metal-driven construction of robust supramolecular arrays.^{1,2} The new assemblies of chromophores, either discrete or polymeric, are investigated for their novel functions, that range from photo-induced processes (i.e., energy and/or electron transfer) to catalysis and molecular recognition. Very often the nature of the peripheral moieties dictates the binding preferences of the porphyrin towards a restricted number of metal ions. For example, pyridyl porphyrins have high affinity for relatively soft metal ions, such as Zn(II), Ru(II) and Re(I), and very low binding constants for 'hard' metal centres such as Sn(IV) or Al(III). On the contrary, carboxyphenylporphyrins bind strongly to Sn(IV) or Al(III) while they have lower affinity for Zn(II), Ru(II) and Re(I). Thus, it is quite obvious that porphyrins bearing two (or more) different peripheral metal-binding sites are particularly appealing, since they allow the selective construction of heteronuclear multi-metal assemblies. Elegant examples in this field were reported by Sanders, Stulz, and co-workers.³

In particular, we are interested in the class of *meso*-pyridyl/carboxyphenyl porphyrins for two main purposes: (i) the construction of multi-metal assemblies by exploiting the different binding affinities of the two functional groups, as explained above, and (ii) the preparation of new water-soluble peripherally-metallated porphyrins to be investigated in medicinal chemistry (e.g., antiviral and anticancer properties). One synthetic approach in this field consists in binding four metal fragments to the peripheral nitrogen atoms of a tetrapyrrolylporphyrin (TPyP). In this case the metal fragments must be highly water soluble and/or charged to impart solubility to the porphyrin conjugate (Fig. 1). We have already prepared a novel water-soluble porphyrin of this kind by binding four charged Ru-nitrosyl fragments, [RuCl₄(NO)]⁻, to Zn·4'-TPyP.⁴ Another synthetic strategy is that of binding the nitrogen atoms of *meso*-pyridyl/carboxyphenyl porphyrins to metal centres and to exploit the deprotonation of the carboxylic groups at physiological pH 7.4 for making the adduct water soluble (Fig. 1). In this case the metal fragment(s) need not to be particularly water soluble and/or charged.

For these reasons we prepared the series of *meso*-(4'-pyridyl)/(4'-carboxymethylphenyl)porphyrins by the 'mixed-aldehyde condensation procedure' under Adler–Longo conditions.⁵ Column chromatography of the mixture afforded four of the *meso*-(4'-pyridyl)/(4'-carboxymethylphenyl)porphyrins in pure form. Ester hydrolysis under basic

* Corresponding author. Tel.: +39 0405587859; fax: +39 04052572; e-mail: gianfer@units.it

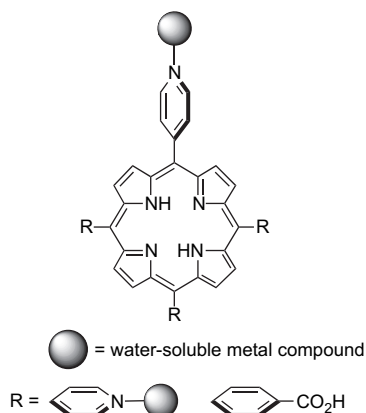


Figure 1. Schematic representation of potentially water-soluble porphyrins peripherally coordinated to metal complexes.

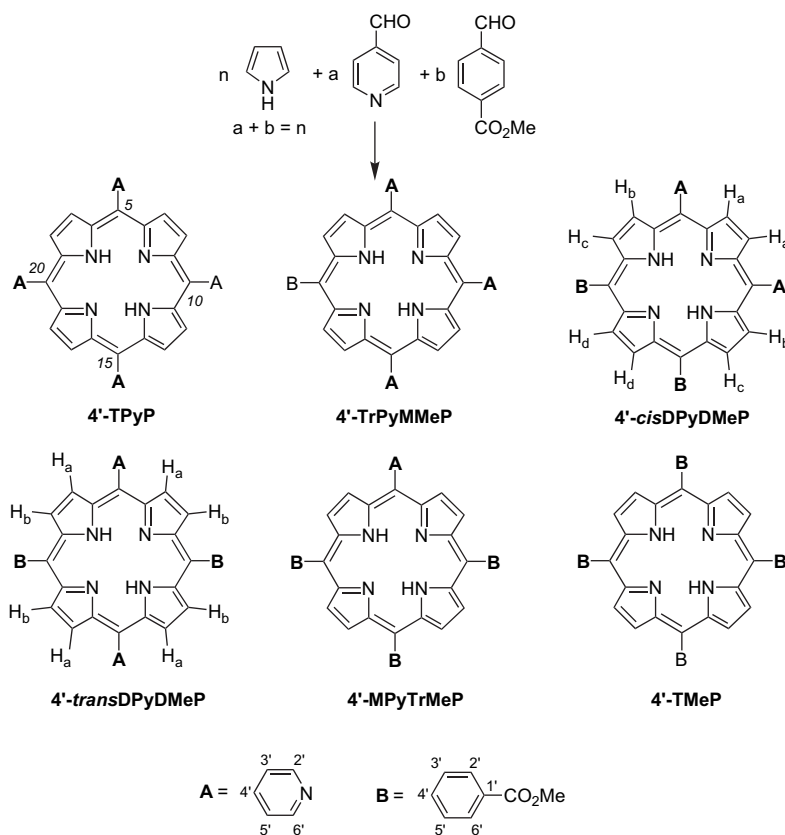
conditions in THF/methanol mixtures, performed on selected isomers, yielded the corresponding *meso*-(4'-pyridyl)/(4'-carboxyphenyl)porphyrins.

In this paper we focus on the two bis-substituted isomeric *meso*-porphyrins, 5,10-bis(4'-pyridyl)-15,20-bis(4'-carboxymethylphenyl)porphyrin and 5,15-bis(4'-pyridyl)-10,20-bis(4'-carboxymethyl-phenyl)porphyrin, respectively, 4'-*cis* and 4'-*trans*DPyDMeP. The possibility of obtaining these two isomeric building blocks in pure form is of great relevance, as they (being carboxylic acids) open the way to the construction of geometrically very different multi-metal supramolecular assemblies of chromophores. Contrary to what

is reported in the literature,⁶ we were able to separate them by TLC and to obtain them in pure form by careful column chromatography. The two geometrical isomers, however, could not be distinguished by conventional spectroscopic techniques. Herein we report their unambiguous NMR characterization that was performed on the trinuclear adducts obtained by selective coordination of [Ru(TPP)(CO)(EtOH)] (TPP=tetraphenylporphyrin) to the peripheral nitrogen atoms. The axially bound ruthenium porphyrins acted as chemical shift reagents and provided a clear distinction of the pyrrole proton resonances of the central porphyrin in the two isomers. Symmetry considerations allowed us to assign the geometry of each isomer. This is an application of a more general method that uses metalloporphyrins as selective chemical shift reagents.

2. Results and discussion

Mixed-aldehyde condensation of pyrrole with 4-pyridylcarboxyaldehyde and methyl 4-formyl benzoate in refluxing propionic acid (Adler–Longo conditions)⁵ yielded, after work-up, a mixture of all six possible *meso*-substituted porphyrins (Scheme 1): tetra-4'-pyridylporphyrin (4'-TPyP), 5,10,15-tris(4'-pyridyl)-20-(4'-carboxymethylphenyl)porphyrin (4'-TrPyMMeP), 5,10-bis(4'-pyridyl)-15,20-bis(4'-carboxymethylphenyl)porphyrin (4'-*cis*DPyDMeP), 5,15-bis(4'-pyridyl)-10,20-bis(4'-carboxymethylphenyl)porphyrin (4'-*trans*DPyDMeP), 5-(4'-pyridyl)-10,15,20-tris(4'-carboxymethylphenyl)porphyrin (4'-MPyTrMeP), and tetra-(4'-carboxymethylphenyl)porphyrin (4'-TMeP).



Scheme 1.

TLC analysis on silica gel, using a dichloromethane/ethanol mixture as eluent, allowed us to resolve five of the six porphyrins in the mixture. Since the pyridyl groups have a higher affinity for silica gel compared to methyl-ester groups, we assumed that 4'-TMeP was eluted first, followed by the tris(4'-carboxymethylphenyl)porphyrin, then by the two bis-substituted geometrical isomers,[†] and finally by the mono-(4'-carboxymethylphenyl)porphyrin. In accordance with this hypothesis, the spot with the highest R_f was unambiguously assigned to 4'-TMeP by comparison with a sample of pure porphyrin obtained by condensation of pyrrole with methyl 4-formyl benzoate. Under our conditions, 4'-TPyP was not eluted. Careful (and often repeated) column chromatography, using different chloroform/ethanol mixtures as eluents, eventually afforded three pyridyl/carboxymethylphenyl porphyrins in pure form.[‡]

The electronic absorption spectra of the products are not diagnostic of the nature and relative geometry of the six-membered rings at the *meso*-positions: they are all very similar and characterized by a strong Soret band at about 418 nm and four Q-bands of decreasing intensities between 512 and 645 nm. Similar considerations apply to the IR spectra. On the contrary, the NMR spectra are diagnostic.

The ¹H NMR spectrum of each porphyrin in CDCl₃ is characterized by typical resonances in the downfield region: two doublets for the pyridyl protons (H2',6'-py and H3',5'-py) and two doublets for the carboxymethylphenyl protons (H2',6'-Ph and H3',5'-Ph), plus a multiplet for the pyrrole β protons (see Scheme 1 for labelling scheme). The spectra also include a singlet for the methyl group(s) at ca. δ=4.1 and one for the NH protons at ca. δ=-2.8. The most downfield resonance was attributed to the pyridyl H2',6' protons, closest to the nitrogen atom. The tris-substituted porphyrin 4'-MPyTrMeP was easily identified by the relative intensities of the pyridyl and carboxymethylphenyl proton resonances (1:3).[‡] However, the spectra of the two bis-substituted geometrical isomers 4'-*cis*DPyDMeP and 4'-*trans*DPyDMeP are almost identical (Fig. 2).

In *meso*-substituted A₂B₂ porphyrins the NMR signals for the pyrrole protons depend on the symmetry and, in principle, might allow the distinction of the *cis*- and *trans*-isomers (provided that the difference in chemical shift between a pyrrole proton adjacent to A and one adjacent to B is such that to make an AX spin system). A *trans*-A₂B₂ porphyrin has two vertical planes of symmetry, while a *cis*-A₂B₂ porphyrin has only one such plane: thus the eight pyrrole protons are expected to give two equally intense doublets (4H each) in the former case, and two doublets plus two singlets (2H each) in the latter (Scheme 1). These two

different NMR patterns are indeed observed for *meso*-(bis)-4'-pyridyl/phenyl porphyrins and allow a clear differentiation of the *cis*- and *trans*-isomers.⁷ However, in the present case, the spin systems of the pyrrole protons are of the AB, rather than AX type (in the magnetic field used), and both geometrical isomers give almost identical multiplets that do not allow to distinguish their geometry (Fig. 2).

Other approaches that, in principle, might be used to distinguish between the two geometries, such as change of solvent, addition of an acid or ¹³C NMR spectroscopy are not useful in this case. In fact, the two isomers are soluble in a narrow range of solvents and typically their spectra are always very similar and do not allow resolution of the pyrrole signals. The addition of an acid would lead to protonation of the inner nitrogens, rather than of the pyridyl nitrogens affording a mixture of products with different degrees of protonation and, in addition, the charge might lead to aggregation and precipitation of porphyrins. A ¹³C NMR experiment should be focused on the number of CH pyrrole resonances: based on symmetry, a *trans*-isomer should have two such resonances and a *cis*-isomer should have four. However, pyrrole carbon resonances are even less sensitive to the nature of the *meso*-six-membered rings than pyrrole proton resonances. Thus, typically it is to be expected that their signals are not sufficiently resolved to allow unambiguous distinction of the two isomers. As anticipated, the ¹³C{¹H} NMR spectra of both 4'-*cis*DPyDMeP and 4'-*trans*DPyDMeP showed the same number and pattern of signals in the aromatic region. In addition, as reported previously for similar systems, the pyrrole carbon resonances are very broad in both isomers and hardly detectable.⁸

Thus, we decided to exploit the reactivity of the two isomers towards [Ru(TPP)(CO)(EtOH)] as a chemical shift reagent. The axial ethanol molecule in [Ru(TPP)(CO)(EtOH)] is weakly bound to ruthenium, and easily replaced by a stronger δ-donor ligand: for example, pyridine replaces ethanol within minutes and makes a strong and inert axial bond with ruthenium. Thus, both the 4'-*cis* and 4'-*trans*DPyDMeP isomers are expected to react selectively through their pyridyl nitrogen atoms (the ester groups are unreactive towards ruthenium) and to bind axially two ruthenium porphyrins, generating the two isomeric side-to-face trimers [(4'-*cis*DPyDMeP){Ru(TPP)(CO)}₂] and [(4'-*trans*DPyDMeP){Ru(TPP)(CO)}₂], that maintain the same symmetry of the parent porphyrin (Fig. 3).

In practice, a CDCl₃ solution of each isomer was titrated with incremental amounts of the commercially available [Ru(TPP)(CO)(EtOH)] and the ¹H NMR spectrum recorded a few minutes after each addition to allow for complete coordination ([Ru(TPP)(CO)(EtOH)] is actually not very soluble in chloroform, but pyridyl coordination brings it in solution). Each titration was stopped when the resonances of the parent porphyrin and of the intermediate dinuclear species disappeared and were replaced by those of the final trinuclear product. As previously observed in similar systems,⁹ the reactions were quantitative, NMR signals were always sharp and no exchange between Ru-coordinated and free porphyrin was observed at NMR concentrations. Signal integration

[†] In principle, the chromatographic retention time might be diagnostic of the geometry of the two bis-substituted geometrical isomers 4'-*cis* and 4'-*trans*DPyDMeP. Since in the case of *meso*-(bis)-4'-pyridyl/phenyl porphyrins the *trans*-isomer was eluted before the *cis* one, it might be argued that also in this case, under very similar chromatographic conditions, the 4'-*trans*DPyDMeP isomer should be eluted first. However, even though reasonable, this argument alone is insufficient for the unambiguous assignment of the two isomers.

[‡] With the ratio between the two aldehydes used in this work, the amount of 4'-TrPyMMeP was always very low and recovery from column chromatography was not pursued (see also Section 4).

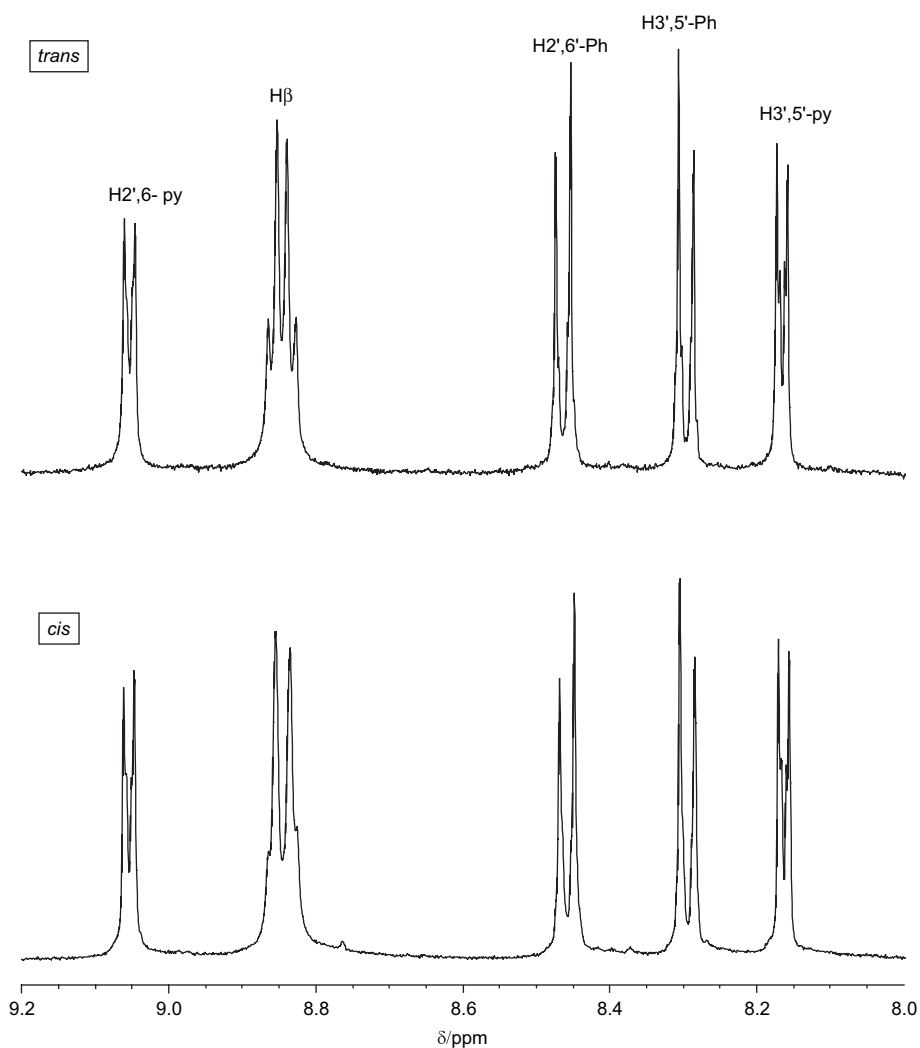


Figure 2. Downfield region of the ¹H NMR spectra (CDCl₃) of 4'-*cis*DPyDMeP (bottom) and 4'-*trans*DPyDMeP (top). See Scheme 1 for labelling scheme.

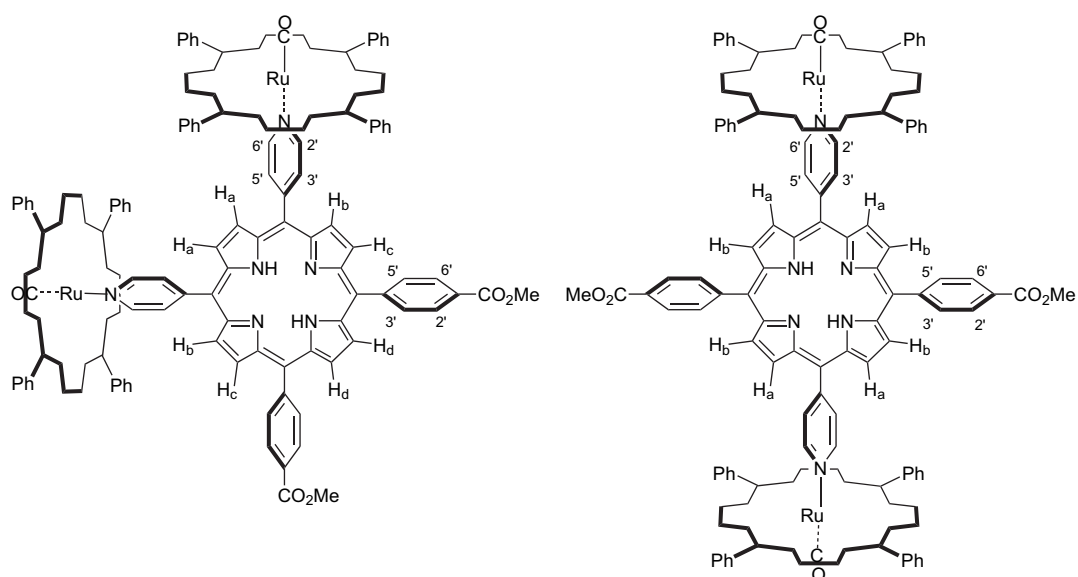


Figure 3. Schematic drawings (with labelling scheme) of the two isomeric side-to-face trimers [(4'-*cis*DPyDMeP){Ru(TPP)(CO)}₂] (left) and [(4'-*trans*DPyDMeP){Ru(TPP)(CO)}₂] (right).

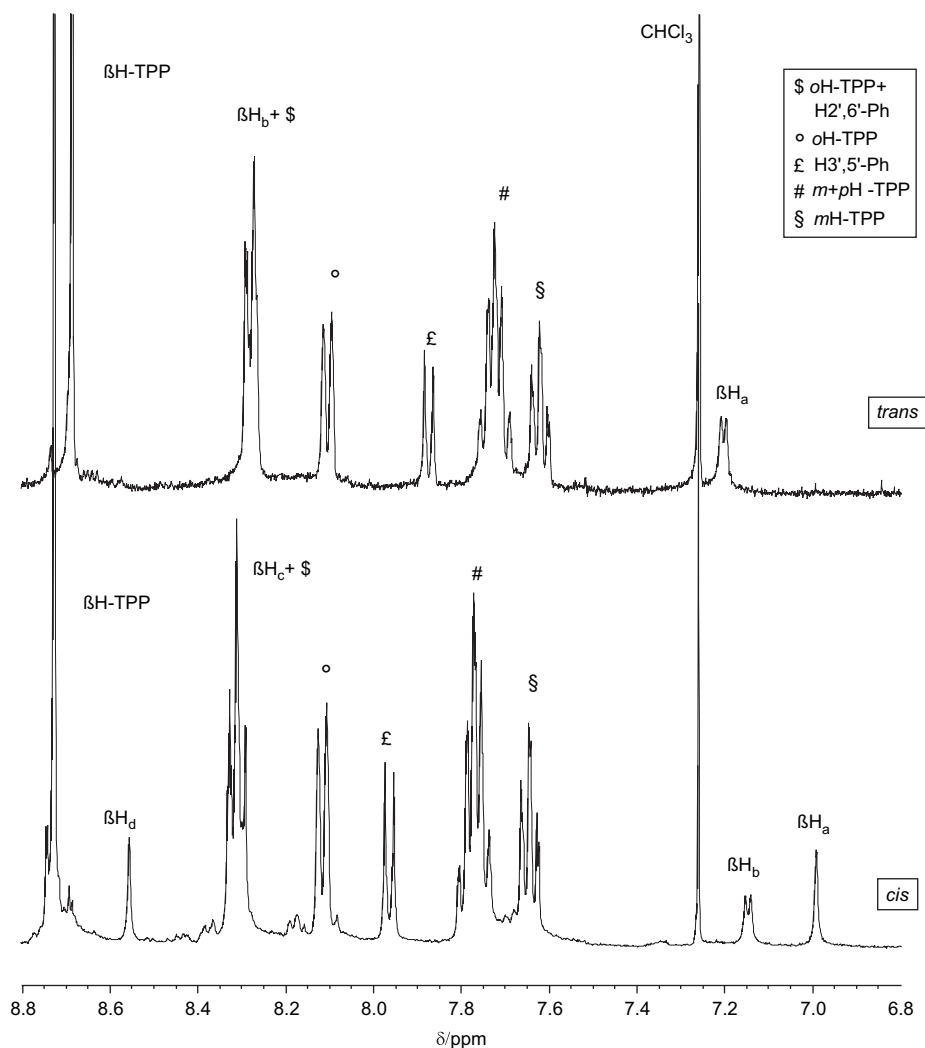


Figure 4. Downfield region of the ^1H NMR spectra (CDCl_3) of $[(4'\text{-cisDPyDMeP})\{\text{Ru}(\text{TPP})(\text{CO})\}_2]$ (bottom) and $[(4'\text{-transDPyDMeP})\{\text{Ru}(\text{TPP})(\text{CO})\}_2]$ (top). See Figure 3 for proton labelling scheme.

confirmed the stoichiometry of the trimeric adducts and signal assignment was supported by 2D H–H COSY experiments.

A common feature in the NMR spectra of axially ligated porphyrin aggregates is the dramatic upfield shift of the resonances of the central porphyrin induced by the (cumulative) anisotropic shielding effect of the peripheral porphyrin(s). The upfield shifts of the NMR resonances of all protons of the central porphyrin are inversely proportional to their distance from the anisotropic shielding of the ruthenium macrocycle (the largest upfield shift was that of the $\text{H}2',6'$ -py protons, from $\delta=9.06$ to $\delta=1.88$ for both adducts). Thus the resonances of the pyrrole protons adjacent to the $4'$ -pyridyl rings, i.e. to the shielding cone of $\text{Ru}(\text{TPP})(\text{CO})$, are expected to be shifted upfield more than those adjacent to the $4'$ -carboxymethylphenyl substituents. The spread of chemical shifts induced by the axial Ru-porphyrins is expected to transform the AB spin systems of the pyrrole protons into an AX system. Indeed, as shown in Figure 4, the pyrrole proton resonances in the NMR spectrum of the trimer containing the bis($4'$ -pyridyl)-bis($4'$ -carboxymethylphenyl)porphyrin eluted first consist of two

well resolved doublets (the most upfield at $\delta=7.20$),[§] thus unambiguously identifying that porphyrin as the *trans*-isomer. Conversely, the pyrrole protons in the trimer containing the isomer with the higher retention time give four equally intense well resolved resonances, two singlets (the most upfield, originated by protons adjacent to the shielding cones of both Ru-porphyrins, at $\delta=6.99$) and two doublets,[§] thus unambiguously qualifying that porphyrin as the *cis*-isomer.

The NMR data, through chemical shift and symmetry arguments, also indicated that at room temperature all the *meso*-six-membered rings experience hindered rotation about the C(*meso*)–C(ring) bond and lie essentially perpendicular to the mean plane of the corresponding porphyrin. Since for the coordinated $\text{Ru}(\text{TPP})(\text{CO})$ chromophores the plane of the porphyrin is not a symmetry plane, the *ortho* and *meta* protons on opposite sites of the phenyl rings experience different magnetic environments and have resolved multiplets.

[§] One doublet overlaps with the $\text{H}2',6'$ -Ph resonances of the $4'$ -carboxymethylphenyl rings and with one set of the phenyl rings of TPP, but was unambiguously identified in the H–H COSY spectrum.

Finally, ester hydrolysis under basic conditions in THF/methanol mixtures¹⁰ afforded 5-(4'-pyridyl)-10,15,20-tris(4'-carboxymethylphenyl)porphyrin in pure form.

3. Conclusions

We demonstrated that each porphyrin in the mixture of *meso*-(4'-pyridyl)/(4'-carboxymethylphenyl)porphyrins, prepared by mixed-aldehyde condensation of pyrrole with 4-pyridylcarboxyaldehyde and methyl 4-formyl benzoate, can be resolved by TLC and most of them can be obtained in pure form by careful column chromatography, including the two bis-substituted *cis* and *trans* geometrical isomers 4'-*cis*DPyDMeP and 4'-*trans*DPyDMeP.

Even though the two isomers could not be distinguished by conventional spectroscopic techniques, their characterization was performed by ¹H NMR spectroscopy on the trinuclear adducts [(4'-*cis*DPyDMeP){Ru(TPP)(CO)}₂] and [(4'-*trans*DPyDMeP){Ru(TPP)(CO)}₂]. In each trimer, the ruthenium chromophores axially bound to the nitrogen-pyridyl moieties acted as chemical shift reagents on the central porphyrin and afforded markedly different patterns for the resonances of its pyrrole protons. Symmetry considerations afforded the final unambiguous correlation of the NMR patterns to the geometry of each isomer. Our method, a simple proton NMR titration that required a few milligrams of each isomeric porphyrin and of the commercially available [Ru(TPP)(CO)(EtOH)], proved to be very helpful and straightforward when more conventional approaches to the resolution of this problem failed.

Finally, we want to stress that this new method is of general applicability for the NMR assignment of the geometry of isomeric porphyrins bearing different peripheral metal-binding functions, provided that the titration is performed with a metalloporphyrin that has high affinity for one of the functions and very little (or no) affinity for the other(s), so that a single multi-porphyrin side-to-face adduct is selectively obtained in each case.

4. Experimental

4.1. General

UV–vis spectra were obtained on a Jasco V-550 spectrophotometer. ¹H and ¹³C NMR spectra were recorded at 400 and 100.5 MHz, respectively, on a JEOL Eclipse 400 FT instrument. All spectra were run at room temperature in CDCl₃ or DMSO-*d*₆ (Aldrich). Proton peak positions were referenced to the peak of residual non-deuterated solvent set at $\delta=7.26$ (chloroform) or 2.50 (DMSO). Assignments were made with the aid of 2D H–H COSY experiments. Carbon signal attributions were based on literature data⁸ and on H–C correlation spectra. Mass spectra (ESI-MS) were recorded on a Bruker ESQUIRE 4000 instrument. Analytical thin-layer chromatography (TLC) was performed on Mackerey-Nagel ADAMANT UV₂₅₄ silica gel pre-coated plates (0.25 mm thick). Column chromatography was performed on silica gel 60 Å (Merck, 230–400 mesh ASTM), eluting with chloroform/ethanol mixtures as specified below. Compounds 4'-TMeP, 4'-MPyTrMeP, 4'-TOHP have been already reported

in literature (see references below). Compounds [(4'-*cis*-DPyDMeP){Ru(TPP)(CO)}₂] and [(4'-*trans*DPyDMeP){Ru(TPP)(CO)}₂] have not been isolated from ¹H NMR titration experiments and no further characterization is given.

4.2. Synthesis and characterization

Pyrrole and 4-pyridylcarboxyaldehyde (Aldrich) were distilled prior to use. The other reactants and solvents were used as received, with the exception of THF that was distilled over LiAlH₄.

4.2.1. *meso*-(4'-Pyridyl)/(4'-carboxymethylphenyl)porphyrins. A mixture of methyl 4-formyl benzoate (3.5 g, 21 mmol) and 4-pyridylcarboxyaldehyde (0.7 mL, 7 mmol) in propionic acid (120 mL) was warmed to 120 °C. Pyrrole (2.0 mL, 28 mmol) was added and the mixture was refluxed for 1.5 h, then stored at –10 °C for 12 h after the addition of ethylene glycol (60 mL). The purple precipitate was removed by filtration, thoroughly washed with cold methanol and dried in vacuo at room temperature. Yield 1.21 g (25%).

Thin-layer chromatography of the crude product (dichloromethane/ethanol 95:5) showed it to be a mixture of the six possible porphyrin isomers: 4'-TPyP, 4'-TrPyMMeP, 4'-*cis*DPyDMeP, 4'-*trans*DPyDMeP, 4'-MPyTrMeP and 4'-TMeP. The *R_f* values of the isomers were

4'-TMeP 0.91,
4'-MPyTrMeP 0.60,
4'-*trans*DPyDMeP 0.55,
4'-*cis*DPyDMeP 0.50,
4'-TrPyMMeP 0.44.

The *R_f* of 4'-TPyP was too small to be measured.

The isomers were separated using column chromatography. To purify large amounts of mixture it was easier to use several columns in series: one large column to remove 4'-TMeP, which constituted approximately 50% of the initial porphyrin mixture, and then smaller columns to separate the other isomers. This mixture of aldehydes (3:1 excess of methyl 4-formyl benzoate) was chosen to obtain the maximum yield of 4'-MPyTrMeP.¹¹ Consequently, 4'-*cis*DPyDMeP, 4'-*trans*DPyDMeP and 4'-TrPyMMeP were obtained in small amounts, so that the isolation of the latter was not pursued; a larger amount of this isomer can be obtained by inverting the relative amounts of the two aldehydes.

Column 1. The column (6×35 cm) was packed with 60 Å silica gel, loaded with 0.63 g of crude porphyrin mixture and eluted with a chloroform/ethanol 98:2 mixture (2 L total). In a typical run, 0.33 g of 4'-TMeP (first band) and 0.29 g of a mixture of 4'-MPyTrMeP, 4'-*cis*DPyDMeP and 4'-*trans*DPyDMeP (second band) were recovered. As noted above, 4'-TrPyMMeP was usually not recovered.

Column 2. Once 4'-TMeP had been removed, it was possible to separate two of the remaining isomers using a smaller column (5×35 cm), packed and eluted as above. A typical separation, starting from 290 mg of crude mixture from column 1, afforded 150 mg of 4'-MPyTrMeP (first band), 110 mg of

a mixture of the three isomers (enriched in 4'-*trans*DPyDMeP and 25 mg of 4'-*cis*DPyDMeP (third band).

Column 3. The 110 mg of mixture from column 2 was loaded on a 4×32 cm column packed and eluted as above. Three fractions were obtained: 4'-MPyTrMeP (50 mg), 4'-MPyTrMeP and 4'-*trans*DPyDMeP (45 mg) and 4'-*cis*DPyDMeP (12 mg).

Column 4. The 50 mg mixture from column 3 was loaded on a 4×27 cm column, packed as above and eluted with a chloroform/ethanol 99:1 mixture (1 L total), affording 17 mg of 4'-MPyTrMeP (first band) and 14 mg of 4'-*trans*DPyDMeP (second band).

The identifications of the porphyrins were confirmed by comparing their R_f values with those of the crude mixture, and by ^1H NMR spectroscopy.

4.2.1.1. 4'-TMeP.⁸ Mp >300 °C. ^1H NMR spectrum (δ , CDCl_3 , see Scheme 1 for labelling scheme): 8.85 (s, 8H, βH), 8.48 (d, $J=8.3$ Hz, 8H, $\text{H}2',6'$), 8.32 (d, $J=8.0$ Hz, 8H, $\text{H}3',5'$), 4.14 (s, 12H, CH_3), -2.80 (s, 2H, NH). UV-vis spectrum (λ_{max} (nm), relative intensity (%)) in CH_2Cl_2 : 420 (100), 515 (4.0), 550 (2.0), 590 (1.4), 646 (1.0). Selected IR spectrum (KBr, cm^{-1}): 3313 (m, ν_{NH}), 1723 (s, $\nu_{\text{C=O}}$), 1276 and 1020 (s, $\nu_{\text{C-O}}$).

4.2.1.2. 4'-MPyTrMeP.⁶ Mp >300 °C. ^1H NMR spectrum (δ , CDCl_3 , see Scheme 1 for labelling scheme): 9.07 (d, $J=5.4$ Hz, 2H, $\text{H}2',6'$ -py), 8.85 (m, 8H, βH), 8.48 (d, $J=8.3$ Hz, 6H, $\text{H}2',6'$ -Ph), 8.32 (d, $J=8.0$ Hz, 6H, $\text{H}3',5'$ -Ph), 8.18 (d, $J=5.9$ Hz, 2H, $\text{H}3',5'$ -py), 4.14 (s, 9H, CH_3), -2.83 (s, 2H, NH). UV-vis spectrum (λ_{max} (nm), relative intensity (%)) in CH_2Cl_2 : 418 (100), 514 (4.5), 549 (1.9), 589 (1.5), 644 (0.8). Selected IR spectrum (KBr, cm^{-1}): 3318 (m, ν_{NH}), 1722 (s, $\nu_{\text{C=O}}$), 1275 and 1020 (s, $\nu_{\text{C-O}}$).

4.2.1.3. 4'-*trans*DPyDMeP. Mp >300 °C. ^1H NMR spectrum (δ , CDCl_3 , see Scheme 1 and Fig. 2 for labelling scheme): 9.06 (d, $J=5.9$ Hz, 4H, $\text{H}2',6'$ -py), 8.85 (m, 8H, βH), 8.46 (d, $J=8.5$ Hz, 4H, $\text{H}2',6'$ -Ph), 8.30 (d, $J=8.3$ Hz, 4H, $\text{H}3',5'$ -Ph), 8.17 (d, $J=5.9$ Hz, 2H, $\text{H}3',5'$ -py), 4.12 (s, 6H, CH_3), -2.87 (s, 2H, NH). ^{13}C NMR spectrum (δ , CDCl_3 , see Scheme 1 and Fig. 2 for labelling scheme): 167.3 (COO), 150.2 ($\text{C}4'$ -py), 148.4 ($\text{C}2',6'$ -py), ca. 147 (v br, $\text{C}\alpha$ -pyrrole), 146.4 ($\text{C}4'$ -Ph), 134.6 ($\text{C}3',5'$ -Ph), ca. 132 (br, $\text{C}\beta$ -pyrrole), 130.0 ($\text{C}1'$ -Ph), 129.5 ($\text{C}3',5'$ -py), 128.1 ($\text{C}2',6'$ -Ph), 119.8 and 117.5 (*Cmeso*), 56.6 (O- CH_3). UV-vis spectrum (λ_{max} (nm), relative intensity (%)) in CH_2Cl_2 : 418 (100), 514 (5.1), 548 (2.1), 589 (1.8), 643 (1.1). MS: (ESI) m/z 733.3 (M^++1).

4.2.1.4. 4'-*cis*DPyDMeP. Mp >300 °C. ^1H NMR spectrum (δ , CDCl_3 , see Scheme 1 and Fig. 2 for labelling scheme): 9.06 (d, $J=5.9$ Hz, 4H, $\text{H}2',6'$ -py), 8.85 (m, 8H, βH), 8.46 (d, $J=8.3$ Hz, 4H, $\text{H}2',6'$ -Ph), 8.30 (d, $J=8.0$ Hz, 4H, $\text{H}3',5'$ -Ph), 8.17 (d, $J=5.9$ Hz, 4H, $\text{H}3',5'$ -py), 4.12 (s, 6H, CH_3), -2.86 (s, 2H, NH). ^{13}C NMR spectrum (δ , CDCl_3 , see Scheme 1 and Fig. 2 for labelling scheme): 167.3 (COO), 150.1 ($\text{C}4'$ -py), 148.4 ($\text{C}2',6'$ -py), ca. 147 (v br, $\text{C}\alpha$ -pyrrole), 146.4 ($\text{C}4'$ -Ph), 134.6 ($\text{C}3',5'$ -Ph), ca. 132

(br, $\text{C}\beta$ -pyrrole), 130.0 ($\text{C}1'$ -Ph), 129.5 ($\text{C}3',5'$ -py), 128.1 ($\text{C}2',6'$ -Ph), 120.0 and 117.4 (*Cmeso*), 56.6 (O- CH_3). UV-vis spectrum (λ_{max} (nm), relative intensity (%)) in CH_2Cl_2 : 418 (100), 514 (4.9), 548 (1.9), 588 (1.7), 644 (0.9). MS: (ESI) m/z 733.3 (M^++1).

4.2.1.5. [(4'-*cis*DPyDMeP){Ru(TPP)(CO)}₂]. ^1H NMR spectrum (δ , CDCl_3 , see Figs. 3 and 4 for labelling scheme): 8.73 (s, 16H, βH -TPP), 8.56 (s, 2H, βH_d), 8.31 (m, 12H, oH -TPP+ $\text{H}2',6'$ -Ph and d, 2H, βH_c partially overlapped), 8.12 (d, $J=7.6$ Hz, 8H, oH -TPP), 7.96 (d, $J=8.3$ Hz, 4H, $\text{H}3',5'$ -Ph), 7.76 (m, 16H, $m\text{H}+p\text{H}$ -TPP), 7.65 (t, $J=7.2$ Hz, 8H, $m\text{H}$ -TPP), 7.14 (d, $J=4.9$ Hz, 2H, βH_b), 6.99 (s, 2H, βH_a), 5.85 (d, $J=6.7$ Hz, 4H, $\text{H}3',5'$ -py), 4.07 (s, 6H, CH_3), 1.88 (d, $J=6.6$ Hz, 4H, $\text{H}2',6'$ -py), -3.78 (s, 2H, NH).

4.2.1.6. [(4'-*trans*DPyDMeP){Ru(TPP)(CO)}₂]. ^1H NMR spectrum (δ , CDCl_3 , see Figs. 3 and 4 for labelling scheme): 8.69 (s, 16H, βH -TPP), 8.28 (m, 12H, oH -TPP+ $\text{H}2',6'$ -Ph and d, 2H, βH_b partially overlapped), 8.10 (d, $J=7.8$ Hz, 8H, oH -TPP), 7.87 (d, $J=8.0$ Hz, 4H, $\text{H}3',5'$ -Ph), 7.73 (m, 16H, $m+p\text{H}$ -TPP), 7.62 (t, $J=7.1$ Hz, 8H, $m\text{H}$ -TPP), 7.20 (d, $J=4.9$ Hz, 4H, βH_a), 5.92 (d, $J=6.8$ Hz, 4H, $\text{H}3',5'$ -py), 4.10 (s, 6H, CH_3), 1.88 (d, $J=6.8$ Hz, 4H, $\text{H}2',6'$ -py), -3.80 (s, 2H, NH).

4.2.2. meso-(4'-Pyridyl)/(4'-carboxyphenyl)porphyrins.

Hydrolysis of the ester groups of meso-(4'-pyridyl)/(4'-carboxymethylphenyl)porphyrins was performed (under basic conditions in THF/methanol mixtures)¹⁰ on the most abundant isomers exclusively, i.e. 4'-TMeP and 4'-MPyTrMeP, and yielded the corresponding meso-(4'-pyridyl)/(4'-carboxyphenyl)porphyrins 4'-TOHP and 4'-MPyTrOHP, respectively. The reactions were monitored by TLC (silica gel, chloroform/ethanol 98:2) until disappearance of the original ester.

4.2.2.1. 4'-TOHP.¹² A 100 mg amount of 4'-TMeP (0.12 mmol) was dissolved in a 2:1 THF/methanol mixture (50 mL). A 40% KOH solution (w/v) (6 mL) was added and the mixture warmed at 40 °C for 30 min under magnetic stirring. At reaction completion, the mixture was acidified to pH 3 with concd HCl and extracted with chloroform (25 mL×3) after addition of water (40 mL). The joined organic fractions were washed with water (20 mL×3) and dried over anhydrous Na_2SO_4 . Solvent removal in vacuo yielded the product as a purple solid (47 mg, 49%). Mp >300 °C. ^1H NMR spectrum (δ , $\text{DMSO}-d_6$, see Scheme 1 for labelling scheme): 13.30 (v br s, 4H, COOH), 8.87 (s, 8H, βH), 8.38 and 8.37 (two partially overlapping doublets, 16H, $\text{H}2',6'$ and $\text{H}3',5'$), -2.94 (s, 2H, NH). UV-vis spectrum (λ_{max} (nm), relative intensity (%)) in ethanol: 416 (100), 513 (4.2), 548 (2.1), 590 (1.3), 646 (0.9).

4.2.2.2. 4'-MPyTrOHP. The same procedure as above was used. A solution of 50 mg amount of 4'-MPyTrMeP (0.063 mmol) in 24 mL of the 2:1 THF/methanol mixture was warmed at 40 °C for 40 h under magnetic stirring after addition of 3 mL of the 40% KOH solution. The work-up afforded the product as a purple solid (24 mg, 51%). Mp >300 °C. ^1H NMR spectrum (δ , $\text{DMSO}-d_6$, see Scheme 1 for labelling scheme): 13.31 (v br s, 3H, COOH), 9.05 (d, $J=5.4$ Hz, 2H, $\text{H}2',6'$ -py), 8.89 (m, 8H, βH), 8.39 (m,

12H, H2',6'-Ph and H3',5'-Ph), 8.29 (d, $J=5.9$ Hz, 2H, H3',5'-py), -2.97 (s, 2H, NH). ^{13}C NMR spectrum (δ , DMSO- d_6): 167.5, 148.3, 145.4, 134.5, 130.5, 129.2, 127.9, 119.4, 117.3. UV-vis spectrum (λ_{max} (nm), $\epsilon \times 10^{-3}$ ($\text{cm}^{-1} \text{M}^{-1}$)) in acetone: 415 (442), 512 (21), 545 (8.4), 589 (6.2), 644 (4.1). MS: (ESI) m/z 748.3 ($\text{M}^+ + 1$).

References and notes

- (a) Chambron, J.-C.; Heitz, V.; Sauvage, J.-P. *The Porphyrin Handbook*; Kadish, K. M., Smith, K. M., Guillard, R., Eds.; Academic: San Diego, CA, 2000; Vol. 6, Chapter 40; (b) Wojaczyński, J.; Grażyński, L.-L. *Coord. Chem. Rev.* **2000**, *204*, 113; (c) Kobuke, Y. *Struct. Bonding* **2006**, *121*, 49; (d) Hupp, J. T. *Struct. Bonding* **2006**, *121*, 145.
- (a) Iengo, E.; Zangrando, E.; Alessio, E. *Eur. J. Inorg. Chem.* **2003**, 2371; (b) Scandola, F.; Chiorboli, C.; Prodi, A.; Iengo, E.; Alessio, E. *Coord. Chem. Rev.* **2006**, *250*, 1471; (c) Iengo, E.; Scandola, F.; Alessio, E. *Struct. Bonding* **2006**, *121*, 105; (d) Iengo, E.; Zangrando, E.; Alessio, E. *Acc. Chem. Res.* **2006**, *39*, 841.
- (a) Sanders, J. K. M.; Bampos, N.; Clyde-Watson, Z.; Darling, S. L.; Hawley, J. C.; Kim, H.-J.; Mak, C. C.; Webb, S. J. *The Porphyrin Handbook*; Kadish, K. M., Smith, K. M., Guillard, R., Eds.; Academic: San Diego, CA, 2000; Vol. 3, pp 1–48; (b) Bouamaied, I.; Coskun, T.; Stulz, E. *Struct. Bonding* **2006**, *121*, 1.
- Gianferrara, T.; Serli, B.; Zangrando, E.; Iengo, E.; Alessio, E. *New J. Chem.* **2005**, *29*, 895.
- Adler, A. D.; Longo, F. R.; Finarelli, J. D.; Goldmacher, J.; Assour, J.; Korsakoff, L. *J. Org. Chem.* **1967**, *32*, 476.
- Sirish, M.; Chertkov, V. A.; Schneider, H.-J. *Chem.—Eur. J.* **2002**, *8*, 1181.
- (a) Meng, G. G.; James, B. R.; Skov, K. A. *Can. J. Chem.* **1994**, *72*, 1894; (b) Alessio, E.; Macchi, M.; Heath, S. L.; Marzilli, L. G. *Inorg. Chem.* **1997**, *36*, 5614.
- Balaban, T. S.; Eichhöfer, A.; Lehn, J. M. *Eur. J. Org. Chem.* **2000**, 4047.
- (a) Alessio, E.; Macchi, M.; Heath, S. L.; Marzilli, L. G. *Chem. Commun.* **1996**, 1411; (b) Iengo, E.; Zangrando, E.; Mestroni, S.; Fronzoni, G.; Stener, M.; Alessio, E. *J. Chem. Soc., Dalton Trans.* **2001**, 1338; (c) Prodi, A.; Chiorboli, C.; Scandola, F.; Iengo, E.; Alessio, E.; Dobrawa, R.; Würthner, F. *J. Am. Chem. Soc.* **2005**, *127*, 1454.
- Luo, C.; Guldi, D. M.; Imahori, H.; Tamaki, K.; Sakata, Y. *J. Am. Chem. Soc.* **2000**, *122*, 6535.
- Lindsey, J. S. *The Porphyrin Handbook*; Kadish, K. M., Smith, K. M., Guillard, R., Eds.; Academic: Boston, MA, 2000; Vol. 1, pp 45–118.
- Harada, A.; Shiotsuki, K.; Fukushima, H.; Yamaguchi, H.; Kamachi, M. *Inorg. Chem.* **1995**, *34*, 1070.